

# How to Directly Measure Floquet Topological Invariants in Optical Lattices

F. Nur Ünal,<sup>1,\*</sup> Babak Seradjeh,<sup>1,2,†</sup> and André Eckardt<sup>1,‡</sup>

<sup>1</sup>Max Planck Institute for the Physics of Complex Systems, Nöthnitzer Straße 38, Dresden 01187, Germany

<sup>2</sup>Department of Physics, Indiana University, 727 E Third Street, Bloomington, Indiana 47405, USA

(Dated: December 12, 2022)

The classification of topological Floquet systems with time-periodic Hamiltonians transcends that of static systems. For example, spinless fermions in periodically driven two-dimensional lattices are not completely characterized by the Chern numbers of the quasienergy bands, but rather by a set of winding numbers associated with the quasienergy gaps. We propose a scheme for measuring these winding numbers in a system of fermionic cold atoms in a periodically driven optical lattice efficiently and directly. It is based on the construction of a one-parameter family of experimentally feasible drives, continuously connecting the Floquet system of interest to a trivial reference system. The winding numbers are then determined by the identification and the tomography of the band-touching singularities occurring on the way. As a byproduct, we also propose a method for probing spectral properties of time evolution operators via a time analog of crystallography.

*Introduction.*—Topological insulators are characterized by integer-valued topological invariants. These are nonlocal bulk properties distinguishing different gapped phases, which change only at energy gap closings, and determine robust properties of the system [1, 2]. For instance, Chern numbers describing generic two-dimensional (2D) band insulators dictate the number of chiral edge modes at the system’s boundary and quantize the Hall response. Thus, the Chern number can be inferred from measuring the Hall response [3, 4], the circular dichroism [5] or by observing chiral edge transport [6–8]. However, a direct measurement of the Chern number characterizing a topologically non-trivial band structure was achieved only very recently [9].

In recent years it was shown that periodically driven (Floquet) systems can also possess robust topological properties [8, 10–30] in ways that transcend static systems [31–33]. While the classification of Floquet topological phases has been established [34, 35] and corresponding anomalous edge modes been observed in photonic systems [28–30], to date a direct measurement of their topological invariants or even a scheme for doing so is lacking. In this paper, we describe how such a direct measurement of Floquet topological invariants can be performed in systems of fermionic atoms in optical lattices.

Consider a generic 2D lattice under time-periodic modulation. The quasistationary Floquet-Bloch states and their quasienergy bands  $\varepsilon_b(\mathbf{k})$ , indexed by  $b$  and quasi-momentum wave vectors  $\mathbf{k}$ , can be obtained from diagonalizing the effective time-independent Floquet Hamiltonian, which generates the stroboscopic evolution of the system in steps of the driving period  $T$ . Like in equilibrium, the bands of the Floquet Hamiltonian can be assigned Chern numbers  $C_b$ . However, these Chern numbers are not sufficient for a complete characterization of the topological properties the Floquet system [31]. The distinction becomes apparent when considering the bulk-boundary correspondence [32]. Since the quasienergies

are defined modulo the drive frequency  $\omega = 2\pi/T$  only, they can be chosen to lie in the Floquet Brillouin zone (FBZ)  $T\varepsilon_b \in (-\pi, \pi]$  (here and after  $\hbar = 1$ ). Defined on a ring, the  $N$  quasienergy bands are separated by  $N$  gaps, where  $N$  denotes the number of basis points in the unit cell. Each quasienergy band gap  $g$  is assigned an integer-valued invariant,  $W_g$ , obtained from the spatiotemporal winding structure of the full time-evolution operator [32]. For a system with an open boundary, the  $N$  independent Floquet topological invariants  $W_g$  count the number of topologically protected chiral edge modes crossing gap  $g$ . Denoting the gap above (below) a band  $b$  with  $>_b$  ( $<_b$ ), one finds  $C_b = W_{>_b} - W_{<_b}$  [32]. As a result, Chern numbers add up to zero when summed over all bands and are described by  $N - 1$  independent integers only. Thus, only for static systems characterized by  $N - 1$  energy gaps Chern numbers provide a full characterization.

In the following, we propose two schemes for directly measuring the winding numbers  $W_g$  in a system of fermionic atoms in a driven optical lattice: A brute-force approach based on the tomography of the full one-cycle evolution operator as well as a much more efficient scheme. The latter relies on the construction of a one-parameter family of drives connecting the Floquet system to a trivial reference point and the identification and the tomography of band-touching singularities occurring in this family. Before describing both schemes, let us introduce the relevant system.

*The system.*—We consider a driven two-dimensional system of spin-polarized fermions in an optical lattice with  $N = 2$  relevant sublattice states per unit cell. It is described by a time-periodic Hamiltonian  $\hat{H}(t) = \hat{H}(t + T)$ , which generates the time-evolution operator  $\hat{U}(t) = \mathcal{T} \exp[-i \int_0^t \hat{H}(t') dt']$  with time ordering  $\mathcal{T}$ . Thanks to the discrete time translation invariance, the stroboscopic evolution of the system over each drive cycle can be described by the time-independent Floquet Hamiltonian  $\hat{H}_F = i \log[\hat{U}(T)]/T$ , whose eigenvalues define the quasienergy spectrum (see, e.g., Ref. [12]). For

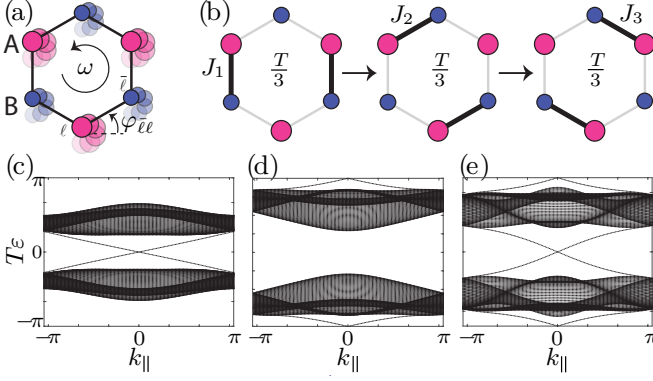


FIG. 1. Driven honeycomb lattice. (a) Continuous drive via circular shaking. (b) Step-wise drive. (c-e) Floquet spectra for continuously driven model on a finite strip with armchair termination, plotted versus the quasimomentum  $k_{\parallel}$  along periodic direction along the strip for  $\nu = 1$ . The parameters are (c)  $\omega = 3J$ ,  $\delta = -2J$ ,  $\kappa = 2$ ; (d)  $\omega = 4J$ ,  $\delta = 0.2J$ ,  $\kappa = 1$ ; (e)  $\omega = 2.5J$ ,  $\delta = -2J$ ,  $\kappa = 1.5$ .

definiteness, the branch of the natural logarithm shall be chosen so that the single-particle quasienergies lie in the FBZ  $(-\omega/2, \omega/2]$ . The winding numbers of the system cannot be extracted just from the Floquet Hamiltonian; they contain information also about the micro-motion, which is captured by the time-periodic operator  $\hat{U}_F(t) = \hat{U}(t)e^{iH_F t}$ .

The Hamiltonian takes the tight-binding form

$$\hat{H}(t) = - \sum_{\langle \ell \ell' \rangle} J_{\ell \ell'}(t) \hat{a}_{\ell'}^{\dagger} \hat{a}_{\ell} + \frac{\Delta}{2} \sum_{\ell} \eta_{\ell} \hat{a}_{\ell}^{\dagger} \hat{a}_{\ell}, \quad (1)$$

where  $\hat{a}_{\ell}$  annihilates a fermion on lattice site  $\ell$ . Each site belongs to one of the two sublattices A or B, for which we define  $\eta_{\ell} = +1$  and  $-1$ , respectively. They are separated by the energy offset  $\Delta = \nu\omega + \delta$ , with the resonant part  $\nu\omega$  and detuning  $\delta$ , where the integer  $\nu$  is chosen so that  $|\delta| \leq \omega/2$ . The time dependency is encoded in the tunneling matrix elements between neighboring sites  $J_{\ell \ell'}(t)$ , which also permit to describe time-periodic conservative forces via modulated Peierls phases  $\arg[J_{\ell \ell'}(t)]$ .

For periodic boundary conditions, the Hamiltonian becomes diagonal with respect to quasimomentum  $\mathbf{k}$ ,

$$\hat{H}(t) = \sum_{\mathbf{k}} \hat{a}_{\mathbf{k}}^{\dagger} \mathcal{H}(\mathbf{k}, t) \hat{a}_{\mathbf{k}}. \quad (2)$$

Here  $\hat{a}_{\mathbf{k}}^{\dagger} = (\hat{a}_{\mathbf{A}\mathbf{k}}^{\dagger}, \hat{a}_{\mathbf{B}\mathbf{k}}^{\dagger})$  is the spinor of fermionic creation operators defined by  $\hat{a}_{\mathbf{s}\mathbf{k}}^{\dagger} = \frac{1}{\sqrt{M}} \sum_{\ell \in \mathbf{s}} e^{i\mathbf{k} \cdot \mathbf{r}_{\ell}} \hat{a}_{\ell}^{\dagger}$ , with  $\mathbf{s} = \mathbf{A}, \mathbf{B}$ , number of unit cells  $M$ , and site positions  $\mathbf{r}_{\ell}$ . The single-particle Hamiltonian  $\mathcal{H}(\mathbf{k}, t)$  can be expressed in terms of the vector of Pauli matrices  $\boldsymbol{\sigma}$  acting in sublattice space,  $\mathcal{H}(\mathbf{k}, t) = \mathbf{h}(\mathbf{k}, t) \cdot \boldsymbol{\sigma}$ . Likewise, we express the time-evolution operator  $\hat{U}(t)$  and the Floquet Hamiltonian  $\hat{H}_F$  in terms of single-particle

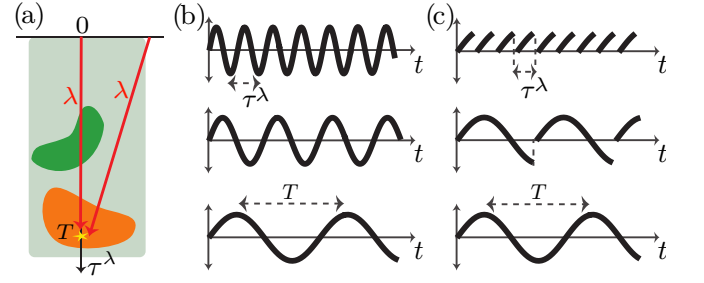


FIG. 2. (a) General scheme of constructing the family of drives. Topologically distinct phases are depicted with different colors in the parameter space given by the drive period  $\tau^{\lambda}$  and other parameters (symbolized by the horizontal axis). Two ways of reaching the target Hamiltonian with period  $T$  [marked by a star in (a)] are: (b) increasing the driving period  $\tau^{\lambda}$  and (c) chopping and repeating the drive at  $\tau^{\lambda}$ .

matrices  $\mathcal{U}(\mathbf{k}, t)$  and  $\mathcal{H}_F(\mathbf{k}) = \mathbf{h}_F(\mathbf{k}) \cdot \boldsymbol{\sigma}$ , respectively. The two quasienergy bands  $\varepsilon_{\pm}(\mathbf{k}) = \pm |\mathbf{h}_F(\mathbf{k})|$  are separated by two gaps, which we label by  $g = 0$  and  $\pi$ :  $\gamma_0(\mathbf{k}) = \varepsilon_{+}(\mathbf{k}) - \varepsilon_{-}(\mathbf{k}) = 2|\mathbf{h}_F(\mathbf{k})|$  is centered around the FBZ center,  $T\varepsilon = 0$ , and  $\gamma_{\pi}(\mathbf{k}) = \omega - \gamma_0(\mathbf{k})$  is centered around the zone edge,  $T\varepsilon = \pi$ .

In order to illustrate our results, we consider two concrete model systems defined on a hexagonal lattice. The first one is driven by a continuous circular force, as it can be realized by lattice shaking [36] [cf. Fig. 1(a)]. It describes recent quantum-gas experiments, where topologically non-trivial band structures were engineered via periodic driving [5, 9, 25, 37, 38]. The force is captured by time-periodic Peierls phases,  $J_{\ell \ell'}(t) = J e^{i\kappa \sin(\omega t - \varphi_{\ell \ell'})}$ , with drive strength  $\kappa$  and polar angle  $\varphi_{\ell \ell'}$  denoting the direction of tunneling. We further assume  $\nu = 1$  which is naturally suitable for state tomography [9, 38]. The second model was introduced in Ref. [31] with  $\nu = 0$ . It is driven in three steps of equal duration  $T/3$ , during each of which the tunneling parameters take a non-zero value  $J$  only along one of the three possible directions [cf. Fig. 1(b)].

The characterization of the driven lattice in terms of winding numbers becomes apparent from Fig. 1(c-e), which shows quasienergy spectra of the continuously driven lattice with momentum  $k_{\parallel}$  along the periodic direction of a strip with armchair termination, for three distinct topologically non-trivial cases. Here each pair of levels traversing the gap with opposite slope corresponds to one chiral edge mode appearing on opposite boundaries of the strip. The insufficient information contained in Chern numbers  $C_{\pm} = \pm(W_{\pi} - W_0)$  becomes apparent by considering the identical values ( $|C_{\pm}| = 1$ ) for the topologically distinct cases shown in subfigures (c) and (d), and their trivial value ( $C_{\pm} = 0$ ) despite the topologically non-trivial situation in subfigure (e).

*Brute-force scheme for measuring  $W_g$ .*—In principle,  $W_g$  may be measured by full tomographic reconstruction

tion of the time-evolution operator  $\mathcal{U}(\mathbf{k}, t)$ . In this brute-force scheme, one has to evolve the system starting from a band-insulating state and perform full state tomography [37, 39] for a sufficiently dense time grid within the drive period. For each quasimomentum  $\mathbf{k}$ , this allows for the reconstruction of both the evolved initial state as well as of the unoccupied state orthogonal to it. However, since each tomography requires another evolution with a flat-band Hamiltonian over a secondary dense time grid, this procedure is rather cumbersome. Moreover, once  $\mathcal{U}(\mathbf{k}, t)$  is obtained approximately, finding  $W_g$  requires further manipulations [32]. A smooth deformation  $\mathcal{U}(\mathbf{k}, t) \rightarrow \mathcal{U}_g(\mathbf{k}, t)$  to a periodic operator  $\mathcal{U}_g(\mathbf{k}, t) = \mathcal{U}_g(\mathbf{k}, t + T)$  is needed that shifts the center of gap  $g$  to  $\pi/T$  for each  $\mathbf{k}$ . Spatiotemporal derivatives of  $\mathcal{U}_g(\mathbf{k}, t)$  have to be estimated from the time and quasimomenta grids. Finally, the invariants can be computed from a discrete approximation of the three-dimensional integral of  $W_g = \frac{1}{8\pi^2} \int dt d^2\mathbf{k} \text{tr}(\mathcal{X}_t^g[\mathcal{X}_{k_x}^g, \mathcal{X}_{k_y}^g])$ , with  $\mathcal{X}_\eta^g = \mathcal{U}_g^{-1} \partial_\eta \mathcal{U}_g$ . The complexity of calculating winding numbers by constructing the evolution operators renders this brute-force approach experimentally challenging. Let us, therefore, present another, more efficient scheme for measuring the winding numbers.

*Efficient scheme.*—The main idea of this scheme is to start in the *high-frequency regime*, which is topologically equivalent to a static system. We then identify a one-parameter family of drives that connects this static Hamiltonian to the target Hamiltonian, whose topology we want to probe. The quasienergy spectrum evolves as we tune through this family and topological transitions occur at quasienergy band touching points. These are topological singularities in the quasienergy spectrum carrying a signed topological charge that defines the change in the topological invariants across the transition. Summing over these topological charges yields the topological invariant associated to each gap of the target Hamiltonian. Therefore, our general scheme consists of: (i) constructing the family of drives connecting the high-frequency regime to the target Hamiltonian; (ii) identifying the band touching points; and (iii) measuring the topological charge of these singularities individually via state tomography. Our scheme is motivated by the classification of Floquet topological insulators via phase bands [33]. However, while phase bands are an abstract theoretical concept, our families of drives can be implemented in concrete experiments. Let us now describe each step in detail.

*Family of drives.*—We first identify the family of Hamiltonians  $\hat{H}^\lambda(t)$  with period  $\tau^\lambda$  by varying a (set of) variable(s), parameterized by  $\lambda \in [0, 1]$ , that map to the target Hamiltonian  $\hat{H}^1(t) = \hat{H}(t)$  with period  $\tau^1 = T$ , see Fig. 2(a). Different choices of  $\hat{H}^\lambda$  take the system through different paths and different sets of topological phase transitions. The key ingredient is that all such paths start at a high-frequency regime with  $\omega^\lambda = 2\pi/\tau^\lambda$

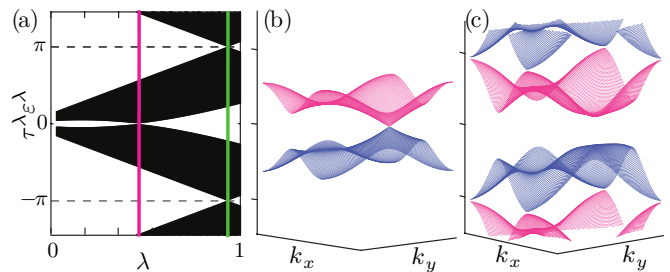


FIG. 3. Quasienergy bands of the circularly shaken honeycomb lattice as the drive frequency is lowered from  $\omega = 10J$  to target frequency  $\omega = 3J$  with drive strength  $\kappa = 1.5$  and sublattice offset  $\Delta = J$ . (b,c)  $\mathbf{k}$ -space plots at topological transitions marked by vertical lines in (a), with topological charges  $q_0 = q_\pi = 1$ .

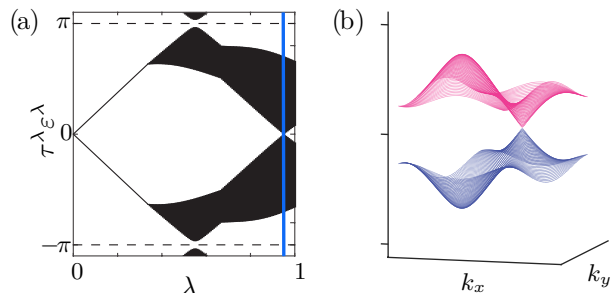


FIG. 4. Quasienergy bands of partial drives constructed for the step-wise drive with  $\omega = 3J$ , and  $\Delta = 0$ , with a topological charge  $q_0 = 1$ .

much larger than the energy scales of the Hamiltonian  $|J(t)|$  and  $|\Delta|$ . As a consequence, one can clearly identify the  $\pi$  gap as the larger gap,  $\gamma_0 \ll \gamma_\pi \sim \omega$ , and conclude that the associated winding number vanishes,  $W_\pi = 0$ . Thus, the topological classification of this initial driven system reduces to that in equilibrium [33], where Chern numbers are sufficient for full characterization. Moreover, for our specific models,  $W_0 = 0$  in the high-frequency regime since all coupling between the bands comes from higher-order corrections [12].

The conditions on  $\tau^\lambda$  are naturally satisfied if we tune the frequency of drive monotonously while keeping the global shape of the drive fixed, as in Fig. 2(b). This corresponds to a parametrization  $\hat{H}^\lambda(t) = \hat{H}(t/\lambda)$ . Alternatively, we also consider a family of drives obtained by chopping the drive after a subperiod time  $\tau^\lambda = \lambda T$  and repeat periodically thereafter. That is,  $H^\lambda(t) = H(t \bmod \tau^\lambda)$ , as depicted in Fig. 2(c).

In Fig. 3(a), we show the evolution of the bulk quasienergy spectrum of a continuously driven lattice as the period is increased up to the target value  $T = 2\pi/3J$  at fixed sublattice offset  $\Delta = J$  and drive strength  $\kappa = 1.5$ . The linear band touchings are zoomed in in Fig. 3(b) and 3(c). On the other hand, Fig. 4 demonstrates the evolution of the quasienergy bands for the

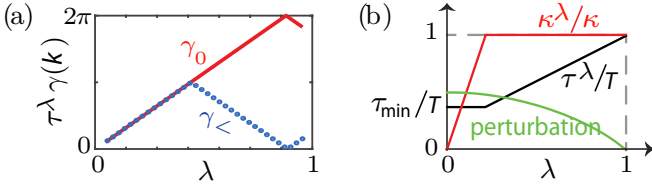


FIG. 5. (a) The measured frequency  $\gamma_<$  at  $\mathbf{k} = 0$  and the quasienergy gap  $\gamma_0$  for the singularity shown in Fig. 3(c). The cusp indicates that the association of the  $\gamma_0$  and the  $\gamma_\pi$  gap as the smaller gap changes. (b) Experimental protocol for the evolution of the system parameters. Starting from a high-frequency with a small period  $\tau^0 \ll |J|, |\Delta|$ , the drive strength  $\kappa^\lambda$  is ramped up to its final value and symmetry-breaking perturbation are smoothly turned off in the target Hamiltonian.

drive-chopping scheme applied to step-wise drive with sublattice offset  $\Delta = 0$  and target period  $T = 2\pi/3J$ . During the first stage of the drive,  $\lambda < 1/3$ , the Hamiltonian is  $\mathbf{k}$ -independent with flat quasienergy bands.

*Identifying singularities.*—We now introduce a protocol for detecting band-touching points of the quasienergy spectrum with respect to  $\lambda$ . For this purpose, one can perform a quench from an arbitrary band insulating state to the Hamiltonian  $\hat{H}^\lambda(t)$ . The stroboscopic evolution in steps of the driving period  $\tau^\lambda$  is governed by the Floquet Hamiltonian  $\hat{H}_F^\lambda$ , which for each quasimomentum  $\mathbf{k}$  defines, a single angular frequency determined by  $2|\mathbf{h}_F^\lambda(\mathbf{k})|$ . Modulo  $\omega^\lambda = 2\pi/\tau^\lambda$  this frequency can be chosen to lie in the interval  $[-\omega^\lambda/2, \omega^\lambda/2]$ , we can measure its absolute value  $\gamma_<^\lambda(\mathbf{k}) \in [0, \omega^\lambda/2]$  by monitoring the evolution of the stroboscopic momentum distribution at momentum  $\mathbf{k}$  [39]. This frequency corresponds to the smaller one of the two band gaps  $\gamma_0^\lambda(\mathbf{k})$  and  $\gamma_\pi^\lambda(\mathbf{k})$ , while the larger one is given by  $\gamma_>^\lambda(\mathbf{k}) = \omega^\lambda - \gamma_<^\lambda(\mathbf{k})$ . In the high frequency limit, we can clearly identify  $\gamma_<^\lambda(\mathbf{k}) = \gamma_0^\lambda(\mathbf{k})$ . Moreover, measuring  $\gamma_<^\lambda(\mathbf{k})$  as a function of  $\lambda$ , one can also identify when this association changes, i.e. when  $\gamma_\pi^\lambda(\mathbf{k})$  becomes smaller than  $\gamma_0^\lambda(\mathbf{k})$  so that  $\gamma_\pi^\lambda(\mathbf{k}) = \gamma_<^\lambda(\mathbf{k})$ . Namely, here  $\gamma_<^\lambda(\mathbf{k})$  reaches a cusp-type maximum at  $\omega^\lambda/2$ , assuming that  $2|\mathbf{h}^\lambda(\mathbf{k})|$  is a smooth function of  $\mathbf{k}$  [cf. Fig. 5(a)]. Once the gaps  $\gamma_g^\lambda$  are measured, one can identify the band touching singularities  $\mathbf{p}^s$  in the three-dimensional parameter space  $\mathbf{p} \equiv (\mathbf{k}, \lambda)$ .

*Measuring topological charge.*—Each singularity carries a topological charge determined by the winding of  $\mathbf{h}_F(\mathbf{p}) \equiv \mathbf{h}_F^\lambda(\mathbf{k})$  around  $\mathbf{p}^s$  in the three-dimensional manifold [33]. For a linear  $g$ -gap closing,  $W_g$  changes by  $q_s = \text{sgn}(\det S) = \pm 1$ , where  $S_{ij} = \partial h_{Fi}/\partial p_j|_{\mathbf{p}^s}$ . We now describe how the matrix  $S$  and the topological charge can be measured experimentally.

To construct  $S$ , we need the Floquet Hamiltonian at six points, in principle, infinitesimally away from the singularity at  $\mathbf{p}^s$ . However, since the topological charge is quantized and therefore protected against small per-

turbations, we can consider the Floquet Hamiltonian at finite distances  $\Delta\mathbf{p}$ . We find that the charge  $q_s$  is extremely robust against the distance  $\Delta\mathbf{p}$  away from a singularity. Deviations occur only when  $\Delta\mathbf{k}$  approaches halfway across the the BZ, and similar rigidity is observed along  $\Delta\lambda$  as evident from the linear profile of the quasienergy in Figs. 3 and 4. While the bands are degenerate at the singularity, they are gapped around it. This allows for an adiabatic state preparation at the six tomography points. Namely, by choosing these points to have a finite distance from  $\mathbf{p}^s$  in quasimomentum (e.g. by displacing them in diagonal  $\mathbf{p}$ -directions from the singularity), they can be reached without gap closing by ramping  $\lambda$ . Moreover, the small- $\lambda$  (high-frequency) regime can be reached from undriven system without crossing a phase transition by smoothly ramping up the driving amplitude. The states so prepared, which contain all the information of the Floquet Hamiltonian at the tomography point, can then be measured via state tomography by suddenly projecting the system onto flat bands [37, 39]. From this information the matrix  $S$  and the topological charge associated with the singularity can be obtained. Once the charges of all the singularities are determined, the topological invariant of each gap  $g$  of the target Hamiltonian is obtained by summing over the charges  $q_g^s$  of the singularities encountered for this gap, while tuning  $\lambda$  from 0 to 1,  $W_g = W_g^0 + \sum_{s_g} q_{s_g}$ . Here  $W_g^0$  is the value of the invariant in the high-frequency regime:  $W_0^0$  equals the Chern number of the high-frequency Hamiltonian, whereas  $W_\pi^0 = 0$ .

*Discussion.*—Some band degeneracies might be extended in the parameter space  $\mathbf{p}$ , due to accidental symmetries [40]. While these extended degeneracies do not pose a problem for the detection of the quasienergy spectrum, they complicate the measurement of topological charges. Fortunately, they can be resolved by adding small symmetry-breaking perturbations as depicted in Fig. 5(b): if indeed there is a singularity hidden in the extended degeneracy, adding such a perturbation would only shift its position in  $\mathbf{p}$  and preserve its topological charge. For example, in Fig. 4(a) there was originally an extended  $\gamma_\pi$ -gap closing, which was resolved by adding a small tunneling anisotropy, so that the tunneling matrix element along one direction was lowered by 20%.

Several remarks are in order regarding the family of drives (cf. Fig. 2). In any realistic experiment, infinite-frequency  $\tau^0 \rightarrow 0$  cannot be attained. In practice, it is sufficient to start from a frequency much larger than  $|J|$  and  $|\Delta|$ , e.g.  $\tau^0 = 2\pi/10J$  in Fig. 3. We sketch such a realistic experimental protocol in Figure 5(b) where in a first step the driving amplitude is ramped from zero to its final value. Also, in the partial drive scheme [cf. Fig. 5(c)], a net force may be induced on the atomic cloud in the optical lattice. In order to prevent atom loss in this case, one can modify the chopped drive by adding



also a constant counter-reacting force to cancel the drift introduced by the truncation.

In the chopped-drive scheme [cf. Fig. 2(c)], the one-cycle evolution operator of the constructed system Hamiltonian directly corresponds to the evolution operator  $\hat{U}(\tau)$  of the target system, with  $\tau < T$ . Thus, the eigenstates of  $\hat{U}(\tau)$  are turned into Floquet modes and the phases of its eigenvalues (corresponding to the phase bands introduced in Ref. [33]) into quasienergies. This allows one to measure the eigenvalues of  $\hat{U}(\tau)$  from the time evolution and to prepare eigenstates of  $\hat{U}(\tau)$  adiabatically. This chopping and repeating of the Hamiltonian in time can be viewed as a time analog of crystallography. Instead of periodically repeating a spatial structure (i.e. crystallizing a complex molecule) for measuring it via diffraction, a temporal structure is repeated for probing its properties. This concept can be generalized to any time evolution generated by a time-dependent Hamiltonian, whether periodic or not.

Finally, we would like to stress that our scheme does not require the adiabatic preparation of the full topological band insulator, but rather relies on the tomography at a number of  $k$ -space points only, making it robust and efficient. It can be a useful tool also for the characterization of topological insulators that are equivalent to static systems, for which  $W_\pi = 0$ . Here a measurement of  $W_0$  directly gives the Chern number  $C_-$  of the lowest band.

This work was supported in part by the National Science Foundation CAREER award DMR-1350663, the US-Israel Binational Science Foundation under grant No. 2014245, the Deutsche Forschungsgemeinschaft via the Research Unit FOR 2414 (grant number EC 392/3-1), and the College of Arts and Sciences at Indiana University. The authors acknowledge fruitful discussions with Robert-Jan Slager and Christof Weitenberg.

---

\* unal@pks.mpg.de

† babaks@indiana.edu

‡ eckardt@pks.mpg.de

- [1] M. Z. Hasan and C. L. Kane, “Colloquium: Topological insulators,” *Rev. Mod. Phys.* **82**, 3045–3067 (2010).
- [2] Xiao-Liang Qi and Shou-Cheng Zhang, “Topological insulators and superconductors,” *Rev. Mod. Phys.* **83**, 1057–1110 (2011).
- [3] K. v. Klitzing, G. Dorda, and M. Pepper, “New method for high-accuracy determination of the fine-structure constant based on quantized hall resistance,” *Phys. Rev. Lett.* **45**, 494–497 (1980).
- [4] Monika Aidelsburger, Michael Lohse, C Schweizer, Marcos Atala, Julio T Barreiro, S Nascimbene, NR Cooper, Immanuel Bloch, and N Goldman, “Measuring the Chern number of Hofstadter bands with ultracold bosonic atoms,” *Nat. Phys.* **11**, 162166 (2015).
- [5] Luca Asteria, Duc Thanh Tran, Tomoki Ozawa, Matthias Tarnowski, Benno S. Rem, Nick Fläschner, Klaus Sen-

- gstock, Nathan Goldman, and Christof Weitenberg, “Measuring quantized circular dichroism in ultracold topological matter,” *arXiv:1805.11077* (2018).
- [6] M. Mancini, G. Pagano, G. Cappellini, L. Livi, M. Rider, J. Catani, C. Sias, P. Zoller, M. Inguscio, M. Dalmonte, and L. Fallani, “Observation of chiral edge states with neutral fermions in synthetic hall ribbons,” *Science* **349**, 1510–1513 (2015).
- [7] B. K. Stuhl, H.-I. Lu, L. M. Ayccock, D. Genkina, and I. B. Spielman, “Visualizing edge states with an atomic bose gas in the quantum hall regime,” *Science* **349**, 1514–1518 (2015).
- [8] Mikael C. Rechtsman, Julia M. Zeuner, Yonatan Plotnik, Yaakov Lumer, Daniel Podolsky, Felix Dreisow, Stefan Nolte, Mordechai Segev, and Alexander Szameit, “Photonic Floquet topological insulators,” *Nature* **496**, 196200 (2013).
- [9] Matthias Tarnowski, F Nur Ünal, Nick Fläschner, Benno S Rem, André Eckardt, Klaus Sengstock, and Christof Weitenberg, “Characterizing topology by dynamics: Chern number from linking number,” *arXiv:1709.01046* (2017).
- [10] Takashi Oka and Hideo Aoki, “Photovoltaic hall effect in graphene,” *Phys. Rev. B* **79**, 081406 (2009).
- [11] Liang Jiang, Takuya Kitagawa, Jason Alicea, A. R. Akhmerov, David Pekker, Gil Refael, J. Ignacio Cirac, Eugene Demler, Mikhail D. Lukin, and Peter Zoller, “Majorana fermions in equilibrium and in driven cold-atom quantum wires,” *Phys. Rev. Lett.* **106**, 220402 (2011).
- [12] André Eckardt, “Colloquium: Atomic quantum gases in periodically driven optical lattices,” *Rev. Mod. Phys.* **89**, 011004 (2017).
- [13] Arijit Kundu and Babak Seradjeh, “Transport signatures of floquet majorana fermions in driven topological superconductors,” *Phys. Rev. Lett.* **111**, 136402 (2013).
- [14] Arijit Kundu, H.A. Fertig, and Babak Seradjeh, “Effective theory of floquet topological transitions,” *Phys. Rev. Lett.* **113**, 236803 (2014).
- [15] Egidijus Anisimovas, Giedrius Žlabys, Brandon M. Anderson, Gediminas Juzeliūnas, and André Eckardt, “Role of real-space micromotion for bosonic and fermionic floquet fractional chern insulators,” *Physical Review B* **91**, 245135 (2015).
- [16] Arijit Kundu, H. A. Fertig, and Babak Seradjeh, “Floquet-engineered valleytronics in dirac systems,” *Physical Review Letters* **116**, 016802 (2016).
- [17] Botao Wang, F. Nur Ünal, and André Eckardt, “Floquet engineering of optical solenoids and quantized charge pumping along tailored paths in two-dimensional chern insulators,” *Phys. Rev. Lett.* **120**, 243602 (2018).
- [18] Mantas Račiūnas, F Nur Ünal, Egidijus Anisimovas, and André Eckardt, “Creating, probing, and manipulating fractionally charged excitations of fractional chern insulators in optical lattices,” *arXiv:1804.02002* (2018).
- [19] Mantas Račiūnas, Giedrius Žlabys, André Eckardt, and Egidijus Anisimovas, “Modified interactions in a floquet topological system on a square lattice and their impact on a bosonic fractional chern insulator state,” *Physical Review A* **93**, 043618 (2016).
- [20] M. Rodriguez-Vega, H. A. Fertig, and B. Seradjeh, “Quantum noise detects floquet topological phases,” *Physical Review B* **98** (2018), 10.1103/phys-

- revb.98.041113.
- [21] M. Rodriguez-Vega and B. Seradjeh, “Universal fluctuations of floquet topological invariants at low frequencies,” *Physical Review Letters* **121** (2018), 10.1103/physrevlett.121.036402.
  - [22] A. R. Kolovsky, “Creating artificial magnetic fields for cold atoms by photon-assisted tunneling,” *EPL (Europhysics Letters)* **93**, 20003 (2011).
  - [23] Alejandro Bermudez, Tobias Schaetz, and Diego Porras, “Synthetic gauge fields for vibrational excitations of trapped ions,” *Phys. Rev. Lett.* **107**, 150501 (2011).
  - [24] Philipp Hauke, Olivier Tieleman, Alessio Celi, Christoph Ölschläger, Juliette Simonet, Julian Struck, Malte Weinberg, Patrick Windpassinger, Klaus Sengstock, Maciej Lewenstein, and André Eckardt, “Non-abelian gauge fields and topological insulators in shaken optical lattices,” *Phys. Rev. Lett.* **109**, 145301 (2012).
  - [25] Gregor Jotzu, Michael Messer, Rémi Desbuquois, Martin Lebrat, Thomas Uehlinger, Daniel Greif, and Tilman Esslinger, “Experimental realization of the topological haldane model with ultracold fermions,” *Nature* **515**, 237 (2014).
  - [26] M. Aidelsburger, M. Atala, M. Lohse, J. T. Barreiro, B. Paredes, and I. Bloch, “Realization of the hofstadter hamiltonian with ultracold atoms in optical lattices,” *Phys. Rev. Lett.* **111**, 185301 (2013).
  - [27] Hirokazu Miyake, Georgios A. Siviloglou, Colin J. Kennedy, William Cody Burton, and Wolfgang Ketterle, “Realizing the harper hamiltonian with laser-assisted tunneling in optical lattices,” *Phys. Rev. Lett.* **111**, 185302 (2013).
  - [28] Wenchao Hu, Jason C. Pillay, Kan Wu, Michael Pasek, Perry Ping Shum, and Y. D. Chong, “Measurement of a topological edge invariant in a microwave network,” *Phys. Rev. X* **5**, 011012 (2015).
  - [29] Fei Gao, Zhen Gao, Xihang Shi, Zhaoju Yang, Xiao Lin, Hongyi Xu, Joannopoulos, Marin Soljacic, Hongsheng Chen, Ling Lu, Yidong Chong, and Baile Zhang, “Probing topological protection using a designer surface plasmon structure,” *Nature Communications* **7** (2016), 10.1038/ncomms11619.
  - [30] Lukas J. Maczewsky, Julia M. Zeuner, Stefan Nolte, and Alexander Szameit, “Observation of photonic anomalous floquet topological insulators,” *Nature Communications* **8** (2017), 10.1038/ncomms13756.
  - [31] Takuya Kitagawa, Erez Berg, Mark Rudner, and Eugene Demler, “Topological characterization of periodically driven quantum systems,” *Phys. Rev. B* **82**, 235114 (2010).
  - [32] Mark S. Rudner, Netanel H. Lindner, Erez Berg, and Michael Levin, “Anomalous edge states and the bulk-edge correspondence for periodically driven two-dimensional systems,” *Phys. Rev. X* **3**, 031005 (2013).
  - [33] Frederik Nathan and Mark S Rudner, “Topological singularities and the general classification of floquet-bloch systems,” *New Journal of Physics* **17**, 125014 (2015).
  - [34] Rahul Roy and Fenner Harper, “Periodic table for floquet topological insulators,” *Physical Review B* **96**, 155118 (2017).
  - [35] Shunyu Yao, Zhongbo Yan, and Zhong Wang, “Topological invariants of floquet systems: General formulation, special properties, and floquet topological defects,” *Physical Review B* **96**, 195303 (2017).
  - [36] André Eckardt, Philipp Hauke, Parvis Soltan-Panahi, Christoph Becker, Klaus Sengstock, and Maciej Lewenstein, “Frustrated quantum antiferromagnetism with ultracold bosons in a triangular lattice,” *EPL* **89**, 10010 (2010).
  - [37] N. Fläschner, B. S. Rem, M. Tarnowski, D. Vogel, D.-S. Lühmann, K. Sengstock, and C. Weitenberg, “Experimental reconstruction of the berry curvature in a floquet bloch band,” *Science* **352**, 1091–1094 (2016).
  - [38] N. Fläschner, D Vogel, M. Tarnowski, B. S. Rem, D.-S. Lühmann, M. Heyl, J. C. Budich, L. Mathey, K. Sengstock, and C. Weitenberg, “Observation of dynamical vortices after quenches in a system with topology,” *Nat. Phys* **14**, 265 (2018).
  - [39] Philipp Hauke, Maciej Lewenstein, and André Eckardt, “Tomography of band insulators from quench dynamics,” *Phys. Rev. Lett.* **113**, 045303 (2014).
  - [40] Conyers Herring, “Accidental degeneracy in the energy bands of crystals,” *Phys. Rev.* **52**, 365–373 (1937).